



National Authority for Remote Sensing and Space Sciences
The Egyptian Journal of Remote Sensing and Space Sciences

www.elsevier.com/locate/ejrs
www.sciencedirect.com



RESEARCH PAPER

Extracting seasonal cropping patterns using multi-temporal vegetation indices from IRS LISS-III data in Muzaffarpur District of Bihar, India



Saptarshi Mondal * , Jeganathan C., Nitish Kumar Sinha, Harshit Rajan, Tanmoy Roy, Praveen Kumar

Department of Remote Sensing, Birla Institute of Technology, Mesra, Ranchi, Jharkhand, India

Received 1 April 2014; revised 11 April 2014; accepted 22 September 2014

Available online 31 October 2014

KEYWORDS

Cropping pattern;
Plantation mapping;
IRS LISS-III image;
Vegetation indices;
Bihar;
India

Abstract The advancement in satellite technology in terms of spatial, temporal, spectral and radiometric resolutions leads, successfully, to more specific and intensified research on agriculture. Automatic assessment of spatio-temporal cropping pattern and extent at multi-scale (community level, regional level and global level) has been a challenge to researchers. This study aims to develop a semi-automated approach using Indian Remote Sensing (IRS) satellite data and associated vegetation indices to extract annual cropping pattern in Muzaffarpur district of Bihar, India at a fine scale (1:50,000). Three vegetation indices (VIs) – NDVI, EVI2 and NDSBVI, were calculated using three seasonal (Kharif, Rabi and Zaid) IRS Resourcesat 2 LISS-III images. Threshold reference values for vegetation and non-vegetation thematic classes were extracted based on 40 training samples over each of the seasonal VI. Using these estimated value range a decision tree was established to classify three seasonal VI stack images which reveals seven different cropping patterns and plantation. In addition, a digitised reference map was also generated from multi-seasonal LISS-III images to check the accuracy of the semi-automatically extracted VI based classified image. The overall accuracies of 86.08%, 83.1% and 83.3% were achieved between reference map and NDVI, EVI2 and NDSBVI, respectively. Plantation was successfully identified in all cases with 96% (NDVI), 95% (EVI2) and 91% (NDSBVI) accuracy.

© 2014 Production and hosting by Elsevier B.V. on behalf of National Authority for Remote Sensing and Space Sciences.

1. Introduction

The 21st century faces multiple challenges like climate change, population growth, food shortage, poverty, hunger, accelerated land cover change and environmental degradation (USCB, 2004; FAO, 2012; IPCC, 2013). World is now filled with more than 7 billion people and the count is increasing at an alarming rate of 1.2% per annum and by 2050 the world

* Corresponding author at: Department of Remote Sensing, Birla Institute of Technology (BIT), Mesra, Ranchi 835215, Jharkhand, India.

E-mail address: sapta.mondal@gmail.com (S. Mondal).

population is projected to reach 9.6 billion (UNFPA, 2012). Due to inadequate food supply, about 1 billion people stay hungry every day in the world and the figure will increase to 2 billion by 2050. This scenario enforces the increasing momentum in agricultural production with more than 70% increase for the developing countries of Asia and Africa in coming decades (FAO, 2009). In this regard, innovative agricultural research and better management practices are essential to enhance productivity. The assessment of crop production and precise and timely monitoring at multi-scale (community level, regional level and global level) have been a challenge to researchers. However, the efficiency and accuracy of crop monitoring have improved significantly since 1972 with the availability of satellite based operational remote sensing acquisition. Globally number of researchers and different government organisations have successfully tested the utilisation of various multi-spectral satellite images at different spatial and temporal scales for agriculture application (MacDonald, 1976; Matthews et al., 1991; Toan et al., 1997; Fang et al., 1999; Ramankutty, 2004; Hannerz et al., 2008; Husak et al., 2008).

The advancement in satellite technology in terms of spatial, temporal, spectral and radiometric resolutions leads to more specific and intensified research on crop classification and discrimination (Van Niel et al., 2004), crop condition simulation and yield estimation (Taylor et al., 1997; Plant et al., 2000; Doraiswamy et al., 2004; Panda et al., 2010; Mkhabela et al., 2011; Bolton et al., 2013), precision farming (Moran et al., 1997; Lamb et al., 2001; Seelan et al., 2003), crop area estimation (Gallego et al., 2014), and crop residue cover mapping (Bannari et al., 2006). Numerous studies were conducted at global to regional scale using coarse to fine spatial resolution multi-temporal data from MODIS, NOAA-AVHRR, LANDSAT, IRS, SPOT, and IKONOS satellite images (Tennakoon et al., 1992; Okamoto and Fukuhara, 1996; Panigrahy et al., 1997; Fang, 1998; Okamoto and Kawashima, 1999; Goward et al., 2003; Prasad et al., 2005; Xiao et al., 2006; Sha et al., 2008; Peng et al., 2011).

Different techniques have been widely demonstrated for agriculture related information extraction and database creation such as classification based mapping (Zhang et al., 1998; Sha et al., 2008; Yang et al., 2011; Saadat et al., 2011), vegetation indices based method (Sun et al., 2000; Yang et al., 2000; Doraiswamy et al., 2003), thresholding method (Xiao et al., 2002a,b; Basnyat et al., 2004; Xiao et al., 2006), and phenology based mapping (Xin et al., 2002; Son et al., 2014). Image classification and index based approaches are straight forward and simple to execute. But most of these are based on single time data analysis and hence possesses uncertainty due to variation (annual and intra-annual) in crop sowing and growth with seasonal fluctuation, and hence unable to quantify annual crop pattern accurately. Through phenology based approach mapping of annual crop cycle and their intensity would be easy, but it requires continuous time series data. For regional level investigation, moderate to fine spatial resolution satellite data are highly required. But the main disadvantage of using fine resolution data is the inadequate availability of good quality continuous data at different phenological stages. Differentiating temporal and spectral variability among various crops during phenological stages are always time consuming and challenging. Also fortnightly time-series satellite data at a

coarse scale resolution (> 500 m) are not useful for fine scale crop mapping. Acquiring fine spatial resolution satellite data at continuous interval is costly and also availability of good quality data is a problem mainly during monsoon period (July–September) in India and hence phenology based approach is not directly utilisable. Amidst this limitation and challenge, the study attempts to extract annual cropping pattern, seasonal cropland types and plantation at a fine scale (1:50,000) through a cost effective and reliable approach, and to understand the effectiveness of different vegetation indices in extracting needed information.

2. Study area and data

Muzaffarpur district is located between $25^{\circ}53'N$ to $26^{\circ}25'N$ and $84^{\circ}50'E$ to $85^{\circ}45'E$ and covers approximately 3172 Sq km area (Census India, 2011). The district has sub-tropical monsoonal climate with annual precipitation of 1207 mm and the winter to summer temperature ranges between $6^{\circ}C$ and $44^{\circ}C$ (Central Ground Water Board (CGWB), 2009). The district experiences three distinct seasons: summer season lasts from April to June, monsoon season lasts from July to October and winter season lasts from November to March. About 70% of total area is arable land (SREP, 2011) and major crops grown in the district are rice, wheat, maize and sugar cane. The district is famous for shahi lychee cultivated in area about 7500 hectare and the average production is about 30,000 tonne per year (Minas et al., 2002). Agriculture and horticulture are the major income source for maximum rural habitant of the district. Fig. 1 represents the locational reference of the study area.

For identifying annual crop-system, multi-temporal Indian Remote Sensing (IRS) Resourcesat-2 LISS III images (path/row: 104/53) were used in this study. Resourcesat-2 has 24 days repetitivity and LISS III data have a spatial resolution of 23.5-m at four spectral bands: Green ($0.52\text{ }\mu\text{m}$ – $0.59\text{ }\mu\text{m}$), Red ($0.62\text{ }\mu\text{m}$ – $0.68\text{ }\mu\text{m}$), NIR ($0.77\text{ }\mu\text{m}$ – $0.86\text{ }\mu\text{m}$) and SWIR ($1.55\text{ }\mu\text{m}$ – $1.70\text{ }\mu\text{m}$). Field survey was carried out in the study area during summer (April 2012) and monsoon seasons (September 2012) in order to know the main crops, their phenology and seasonal cropping pattern. It was found that the main cropping seasons in this area are Kharif season (July–August to September–October), Rabi season (December–January to February–March) and Zaid season (March–April to May–June). These three seasons form three type of cropping period: (i) single seasonal (Kharif, Rabi and Zaid), (ii) double seasonal (Kharif-Rabi, Kharif-Zaid and Rabi-Zaid) and (iii) triple seasonal (Kharif-Rabi-Zaid). Fig. 2 depicting the annual crop phase of major crops cultivated in Muzaffarpur district.

Based on the ground knowledge and cropping pattern we acquired three satellite data during March, May and October so as to cover correct cropping pattern and to differentiate plantation. Table 1 reveals the details about the three satellite data and their date of acquisition.

3. Methodology

In this study multi-seasonal satellite images and VI were used for large area seasonal crop mapping. Fig. 3 provides the overall processes followed in this study.

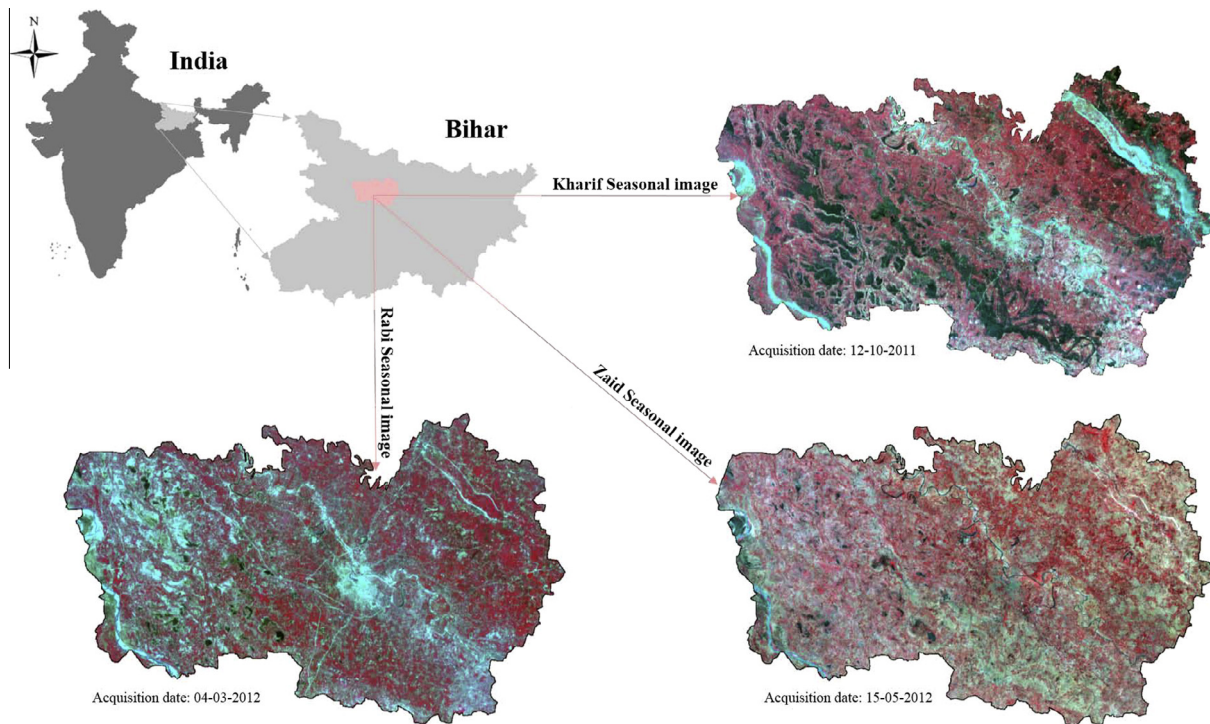


Figure 1 Location map of Muzaffarpur district, Bihar.

3.1. Reference cropping pattern extraction through visual interpretation

Initial geo-referencing was carried out to bring three satellite data into a same locational framework. Manual digitisation was performed using standard FCC from three seasonal images to extract eight different vegetation classes: (i) three single seasonal crop classes (Kharif, Rabi and Zaid); (ii) three double seasonal crop classes (Kharif-Rabi, Kharif-Zaid & Rabi-Zaid); (iii) one triple seasonal crop class (Kharif-Rabi-Zaid) and (iv) plantation. Classification process of multi-temporal LISS III image was carried out by following three steps. First, a base layer was created from kharif season FCC image and all the vegetation classes during kharif season were identified. Second,

the base layer was updated using Rabi season FCC image. All kharif crop clusters having crop in Rabi season were identified as double cropland (Kharif-Rabi). Third, the information from kharif and Rabi seasons was updated using zaid season FCC image and the combination of double cropland (Kharif-zaid & rabi-zaid) and triple cropland (kharif-rabi-zaid) and plantation was delineated correctly.

3.2. Semi-automated cropping pattern extraction using temporal vegetation indices

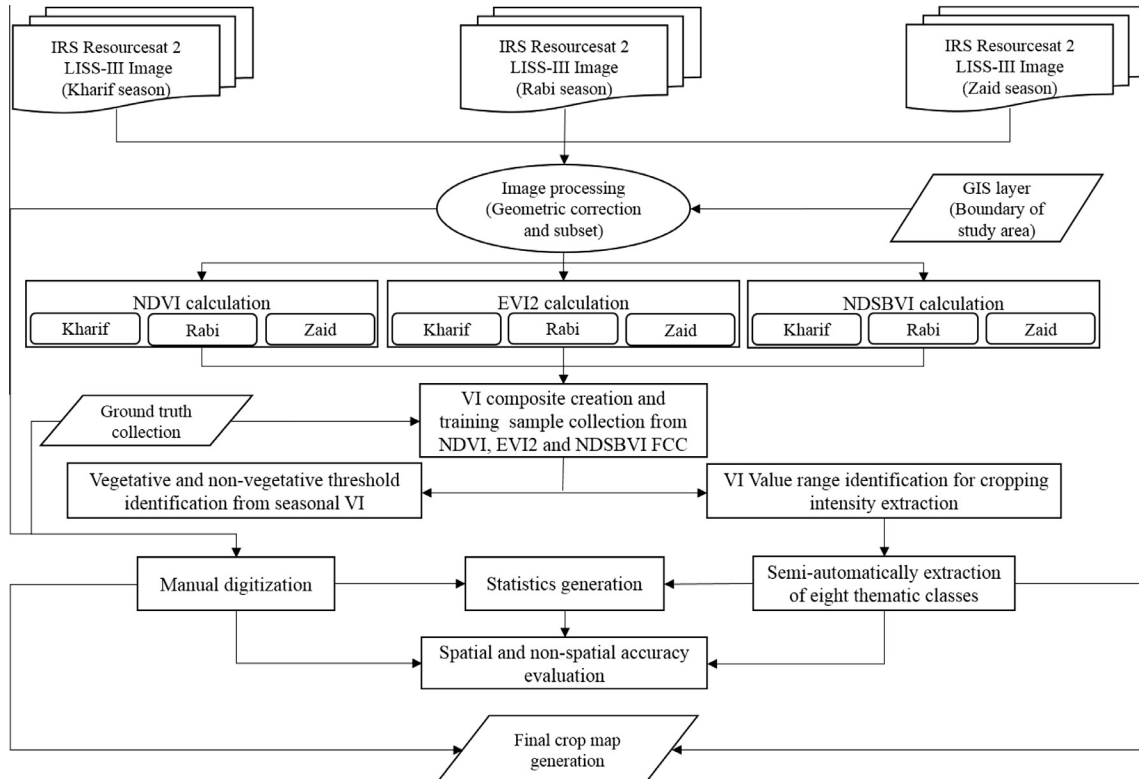
Three different vegetation indices: Normalised differential Vegetation Index (NDVI), two band Enhanced Vegetation Index (EVI2) & Normalised differential Short wave-infrared

Crop	Crop Phase	Jan	Feb	Mar	Apr	May	Jun	Jul	Aug	Sep	Oct	Nov	Dec
		I	II	III									
Rice (Garma/Boro)	Planting												
	Developing												
	Harvesting												
Rice (Shahi/Aghani)	Planting												
	Developing												
	Harvesting												
Wheat	Planting												
	Developing												
	Harvesting												
Maize	Planting												
	Developing												
	Harvesting												
Sugarcane	Planting												
	Developing												
	Harvesting												
Lychee	Flowering												
	Fruiting												
	Harvesting												
Mango	Flowering												
	Fruiting												
	Harvesting												

Figure 2 Major Crop Calendar of Muzaffarpur District.

Table 1 Details of IRS Resourcesat-2 LISS-III image used in the study.

Satellite and sensor name	Path/row No.	Season name	Acquisition date
IRS Resourcesat-2 LISS-III	104/54	Kharif season	12th October 2011
		Rabi season	4th March 2012
		Zaid season	15th May 2012

**Figure 3** Flowchart of the methodology showing the steps of data processing used in the study.

based vegetation Index (NDSBVI) were used for automatic extraction of annual cropland types and to discriminate plantation from crop. These indices use the reflectance value from Red ($0.62\text{ }\mu\text{m}$ – $0.68\text{ }\mu\text{m}$), NIR ($0.77\text{ }\mu\text{m}$ – $0.86\text{ }\mu\text{m}$) and SWIR ($1.55\text{ }\mu\text{m}$ – $1.70\text{ }\mu\text{m}$) bands of IRS Resourcesat-2 LISS III images. Three sets of these indices were calculated for three different seasons. NDVI is based on the simple ratio of difference and sum of NIR and red band reflectance values, and the most accepted vegetation index for identifying vegetative vigour. EVI is an improved vegetation index than NDVI as canopy background-adjustment factor used for reducing background soil noise, and in addition, it is very sensitive to biomass. IRS LISS III sensor do not have Blue band and hence a modified EVI method utilising red and NIR bands was adopted in this study as recommended by Jiang et al. (2008). SWIR band is sensitive to leaf water content and useful for plant water stress and leaf moisture content estimation and hence, Normalised differential Short Wave-infrared based vegetation index (NDSBVI) was used in this study.

$$NDVI = \frac{(\rho_{nir} - \rho_{red})}{(\rho_{nir} + \rho_{red})}$$

(Rouse et al., 1973)

$$EVI2 = \frac{2.5 * (\rho_{nir} - \rho_{red})}{(\rho_{nir} + 2.4 * \rho_{pred} + 1)}$$

(Jiang et al., 2008)

$$NDSBVI = \frac{(\rho_{swir} - \rho_{pred})}{(\rho_{swir} + \rho_{pred})}$$

(Thenkabail et al., 1995)

where,

ρ_{pred} = Reflectance of RED band,

ρ_{nir} = Reflectance of Near-infrared band and

ρ_{swir} = Reflectance of Short wave-infrared band.

The VI value ranges in an image depend upon the growth stage (i.e., phenology) of different vegetation species, environmental factors, topography and sun-sensor geometry. In this study, a detailed sampling (training clusters) was done over the VI images from three different seasons for finding the threshold value of vegetation and non-vegetation classes. The VI value range obtained for different classes using samples were applied over the full VI annual image stacks of [NDVI stack – ndvi(k), ndvi(r), ndvi(z); EVI stack – evi(k), evi(r),

evi(z); NDSBVI stack – ndsbvi(k), ndsbvi(r), ndsbvi(z)]as conditional function, separately to extract full spatial presence of each class. This process resulted into three different classified images, one each from NDVI, EVI and NDSBVI. Finally, the accuracy of these three results was evaluated with respect to reference-digitised map.

4. Results and discussion

The three multi-seasonal satellite images collected from IRS LISS III data could be seen in Fig. 1. In standard FCC the cropping area appears as pink to red in all three seasons (Kharif, rabi and zaid) and plantation area appears as deep red in kharif and zaid seasons and blackish in rabi season. It could be seen that most of the plantation areas were in close proximity with cropping areas. It was observed that spectral responses of plantation canopy were similar to those of crop canopy during kharif and zaid seasons, and hence it was difficult to differentiate plantation from crop most of the time. However, spectral behaviour of plantation was different from crops during rabi season. Hence, for accurate mapping of cropland and plantation, multi-season satellite images are required. Lychee and Mango plantation are mainly grown in this region of Bihar as the study area is the leading exporter of Shahi Lychee in India. A reference-classified map depicting various crop types and pattern was generated by manual digitisation using three seasonal standard FCC. During classification minimum mappable unit (MMU) was considered as 2.5 hectare to avoid too many small cluster. Clusters having mixed classes often create confusion to classify a particular class. Therefore, a cluster having 75% of homogeneous class was considered as a single class. Plantation clusters were delineated using images of all

seasons simultaneously. Because, in kharif and zaid seasons plantation having similar signature of crop and in rabi season plantation having similar signature of settlement often create confusion during interpretation which increases the chances of misinterpretation. In addition, it was difficult to use multi-season images during visual interpretation, as we need to switch between multiple images to understand the type of crop and its areal extent in a correct manner. To effectively integrate multi-seasonal satellite images and to extract the cropping pattern in a semi-automated manner, the study used VI stacks from different seasons and evaluated their accuracy of mapping. Fig. 4 reveals the seasonal stacks from different VI images.

FCC using seasonal NDVI, EVI2 and NDSBVI (Fig. 4a–c) was found to be very effective in revealing seasonal components of various vegetation classes. It could be seen from Fig. 4 that single seasonal crops (Kharif, Rabi and Zaid) were represented as red, green and blue colour respectively. Double cropping areas were represented by three additive colours: yellow (kharif and rabi), magenta (kharif and zaid) and cyan (rabi and zaid); and triple cropping areas were represented as white colour.

Total 40 training clusters (five sample clusters for each class) were collected, and VI value ranges and associated statistics (minimum, maximum, mean and standard deviation) were estimated for vegetation and non-vegetation classes. Table 2 provides the exact value ranges and statistics derived from the training clusters for NDVI, EVI2 and NDSBVI at different seasons. Fig. 5 provides the graphical variation in the VI values for different classes. Single (Kharif, Rabi and Zaid), double (kharif-rabi, kharif-zaid and rabi-zaid) and triple cropping period were represented by the curves having one peak, two

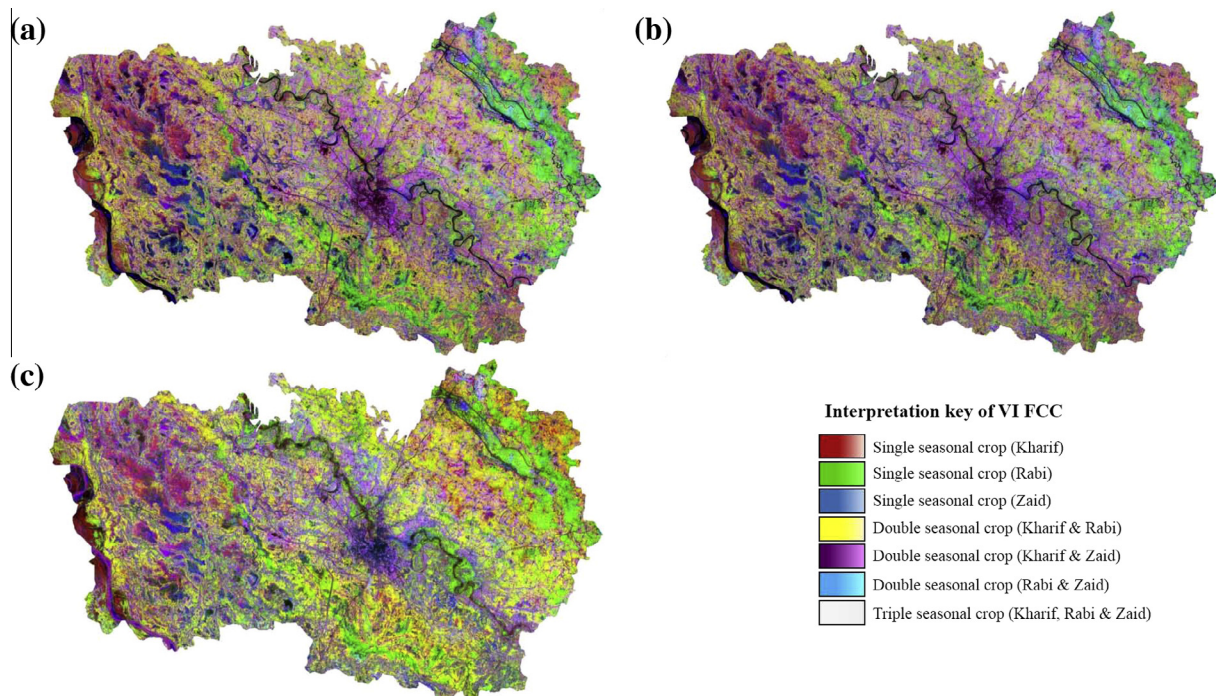


Figure 4 FCC of stacked seasonal (Red band-Kharif, Green band-Rabi & Blue band-Zaid) VI layers – (a) NDVI, (b) EVI2 and (c) NDSBVI (interpretation keys were used for sample collection).

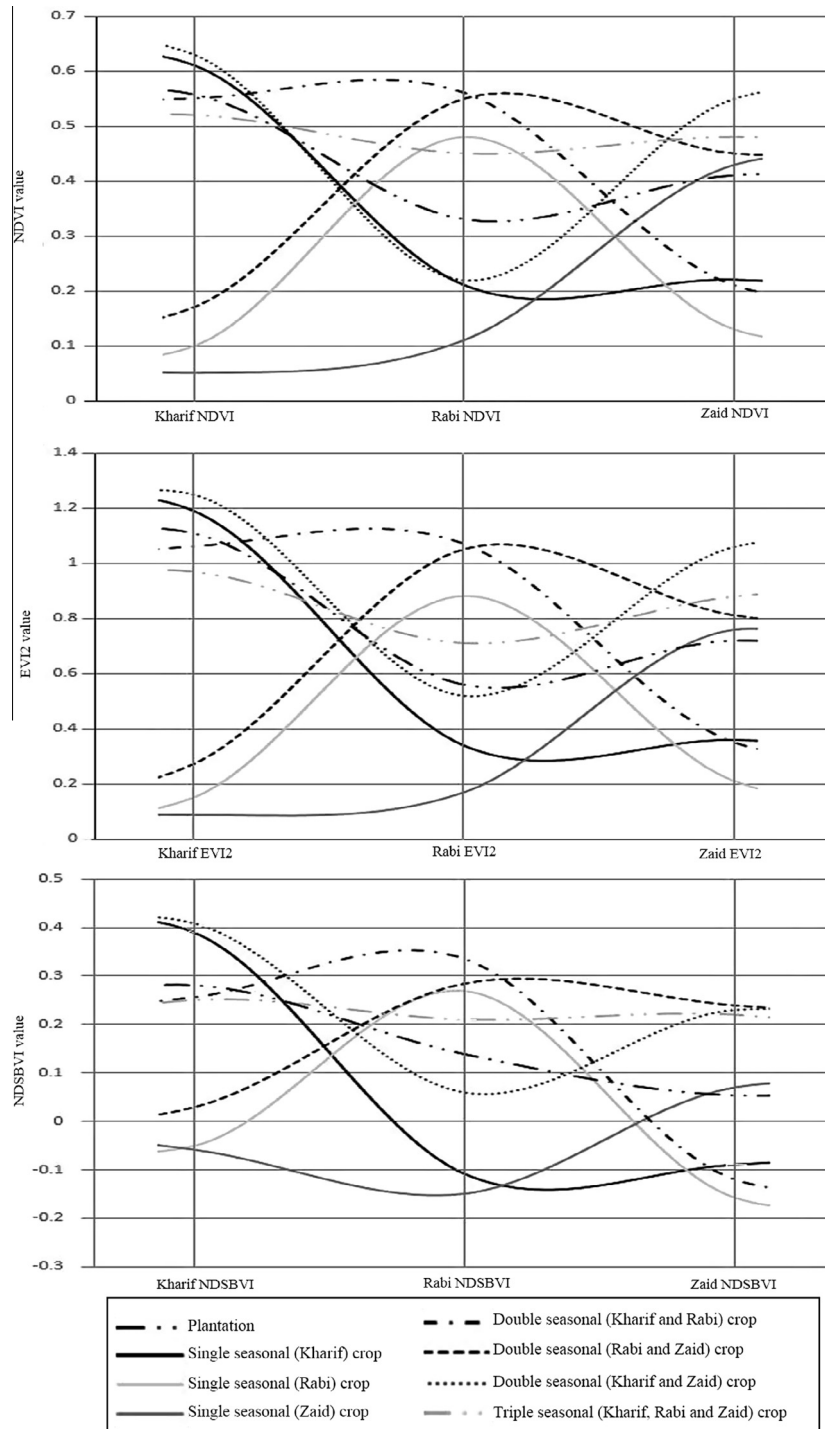


Figure 5 Characteristics curve of various cropping types using seasonal VI data based on (a) NDVI, (b) EVI2 and (c) NDSBVI.

peak and three peak respectively in NDVI, EVI2 and NDSBVI. For plantation, the VI curve exhibits a quite different shape than crops when all the seasons were considered.

These values were grouped into three broader classes: crop, plantation and others, and their value ranges were graphically represented in Fig. 6 to get a broad understanding about seasonal variation in VI value ranges in NDVI, EVI2 and NDSBVI.

The threshold values for vegetation and non-vegetation pixel were estimated using NDVI, EVI2 and NDSBVI during

each season (Kharif, Rabi and Zaid). The NDVI threshold value for vegetative pixels was found as >0.39 in Kharif, >0.23 in Rabi and >0.25 in Zaid. In addition, the value range for crop and plantation was also estimated (Fig. 6a). An overlapping NDVI value range was found for crop and plantation during Kharif and Zaid seasons. However, distinct VI ranges were identified for plantation ($>0.23 - <0.41$) and crop ($>0.41 - <0.67$) in NDVI during rabi (see Fig. 5a). The EVI2 threshold value for vegetation was >0.59 in Kharif, >0.37 in Rabi and 0.49 in Zaid season. In EVI, two distinct ranges

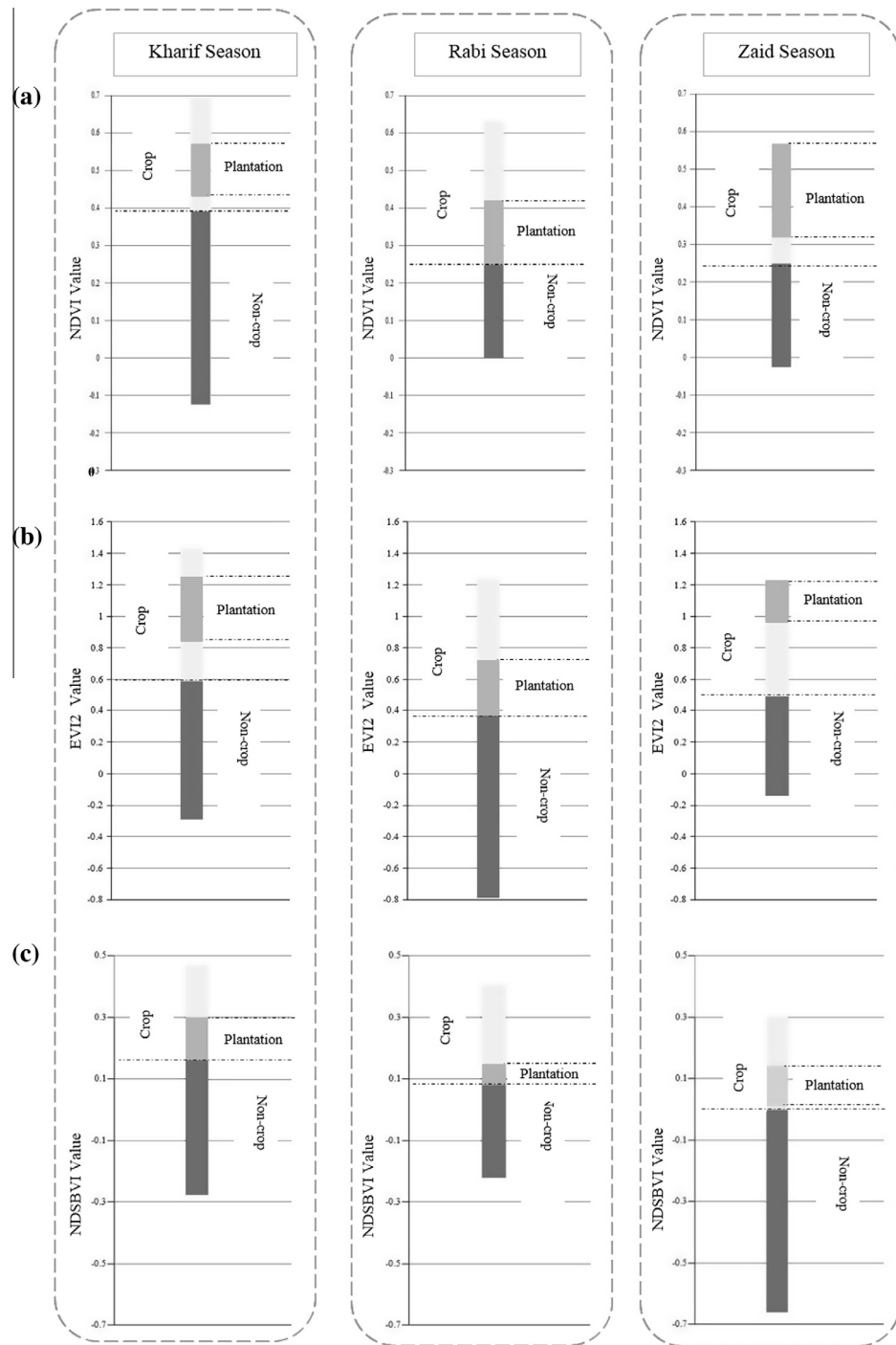


Figure 6 Simplified depiction of VI value range for crops, plantation and non-crop classes obtained using samples from seasonal VI stacks of (a) NDVI, (b) EVI and (c) NDSBVI.

were found for crop ($> 0.72 - < 1.24$) and plantation ($> 0.37 - < 0.72$) during rabi, but an overlapping range was found during kharif and zaid seasons (Fig. 6b). Interestingly, the overall value range in NDSBVI was much lower than NDVI and EVI2 in all the seasons. In NDSBVI, the threshold value for vegetation was identified as > 0.16 in kharif, > 0.08 in Rabi and > 0.03 in Zaid season. NDSBVI was capable of discriminating crop and plantation during both kharif and rabi, unlike NDVI

and EVI2. The value ranges in NDSBVI during kharif and rabi for plantation are $> 0.16 - < 0.3$, $> 0.08 - < 0.15$ and $> 0.3 - < 0.47$, $> 0.15 - < 0.406$ for crop, respectively. However, in Zaid season there was an overlapping value range between crop and plantation (Fig. 6c).

A conditional decision operation was made using the VI value ranges provided in Table 2 in order to extract various crop types and its patterns. For example, following conditions

Table 2 Seasonal Crop VI value statistics estimated from 40 training samples.

Crop type	NDVI			EVI2			NDSBVI			
	Kharif	Rabi	Zaid	Kharif	Rabi	Zaid	Kharif	Rabi	Zaid	
Plantation	Min	0.43	0.23	0.32	0.84	0.37	0.49	0.12	-0.01	0.01
	Max	0.66	0.42	0.57	1.25	0.72	0.96	0.30	0.15	0.14
	Mean	0.54	0.33	0.45	1.05	0.55	0.73	0.21	0.07	0.08
	SD	0.16	0.13	0.18	0.29	0.25	0.33	0.13	0.12	0.09
Single crop (Kharif)	Min	0.39	0.12	-0.85	0.59	0.17	0.13	0.17	-0.08	-0.14
	Max	0.66	0.31	0.25	1.43	0.46	0.59	0.47	0.10	0.00
	Mean	0.52	0.21	-0.30	1.01	0.32	0.36	0.32	0.01	-0.07
	SD	0.19	0.14	0.78	0.59	0.21	0.33	0.21	0.12	0.10
Single crop (Rabi)	Min	-0.14	0.36	0.08	-0.21	0.74	0.15	-0.12	0.17	-0.17
	Max	0.37	0.62	0.25	0.75	1.24	0.51	0.17	0.41	-0.04
	Mean	0.12	0.49	0.17	0.27	0.99	0.33	0.02	0.29	-0.11
	SD	0.36	0.18	0.12	0.68	0.35	0.25	0.21	0.17	0.09
Single crop (Zaid)	Min	0.10	0.11	0.25	-0.21	0.17	0.51	-0.10	-0.12	0.00
	Max	0.39	0.25	0.57	0.75	0.51	1.23	0.09	0.08	0.30
	Mean	0.24	0.18	0.41	0.27	0.34	0.87	0.00	-0.02	0.15
	SD	0.21	0.10	0.23	0.68	0.24	0.51	0.13	0.14	0.21
Double crop (Kharif & Rabi)	Min	0.39	0.36	0.08	0.59	0.17	0.49	0.17	0.12	-0.17
	Max	0.66	0.62	0.25	1.43	0.72	1.23	0.47	0.41	0.01
	Mean	0.52	0.49	0.17	1.01	0.44	0.86	0.32	0.27	-0.08
	SD	0.19	0.18	0.12	0.59	0.39	0.52	0.21	0.21	0.13
Double crop (Kharif & Zaid)	Min	0.39	0.11	0.25	1.25	0.17	0.51	0.30	-0.09	0.01
	Max	0.66	0.25	0.57	1.43	0.72	1.23	0.47	0.22	0.30
	Mean	0.52	0.18	0.41	1.34	0.45	0.87	0.39	0.07	0.16
	SD	0.19	0.10	0.23	0.13	0.39	0.51	0.12	0.22	0.21
Double crop (Rabi & Zaid)	Min	-1.35	0.36	0.25	0.18	0.74	0.51	-0.10	0.12	-0.04
	Max	0.39	0.62	0.57	0.59	1.24	1.23	0.12	0.41	0.30
	Mean	-0.48	0.49	0.41	0.39	0.99	0.87	0.01	0.26	0.13
	SD	1.23	0.18	0.23	0.29	0.35	0.51	0.15	0.21	0.24
Triple crop (Kharif, Rabi & Zaid)	Min	0.39	0.42	0.25	0.59	0.74	0.51	0.17	0.22	0.01
	Max	0.66	0.62	0.57	1.43	1.24	1.23	0.47	0.41	0.30
	Mean	0.52	0.52	0.41	1.01	0.99	0.87	0.32	0.32	0.16
	SD	0.19	0.14	0.23	0.59	0.35	0.51	0.21	0.13	0.21

were implemented to extract kharif class and plantation from seasonal NDVI stack:

Single seasonal (Kharif) crop

$$= \text{Con}\{(\text{Kharif_NDVI} > 0.39 \& \text{Kharif_NDVI} \leq 0.66) \& (\text{Rabi_NDVI} > 0.12 \& \text{Rabi_NDVI} \leq 0.39) \& (\text{Zaid_NDVI} > -0.85 \& \text{Zaid_NDVI} \leq 0.25)\}$$

Plantation

$$= \text{Con}\{(\text{Kharif_NDVI} > 0.43 \& \text{Kharif_NDVI} \leq 0.66) \& (\text{Rabi_NDVI} > 0.23 \& \text{Rabi_NDVI} \leq 0.42) \& (\text{Zaid_NDVI} > 0.32 \& \text{Zaid_NDVI} \leq 0.57)\}$$

where,

Con = Condition.

Similar conditions were applied for all other classes. Fig. 7 reveals the output classified images using seasonal NDVI stack (Fig. 7b), EVI stack (Fig. 7c) and NDSBVI stack (Fig. 7d).

The resultant area statistics using all the classified images were extracted and were compared (spatially and non-spatially) with reference digitised classification statistics (Table 3).

Non-spatially, among the three VIs, NDVI was found to show better area estimate having close agreement with reference area. The total vegetated area in the classified maps from visual interpretation, NDVI, EVI2 and NDSBVI was 2207 Sq km, 1900 Sq km, 1836.8 Sq km and 1839 Sq km, respectively. Single season (kharif) crop class, single season (zaid) crop class and triple season crop class were observed having greater area in all VIs than reference area. In addition, single season (Rabi) crop, Double season crop and plantation have lesser area in all VIs than reference area. In visual classification, a class was identified by digitising the cluster having 70% homogeneous pixel and hence, 30% of heterogeneous mixed pixels were also included into a particular class which causes over-estimate of area in a particular class. Also due to MMU limit the entire small cluster having area of < 2.5 hectare was merged into neighbour cluster and hence causing under-estimate about these smaller patch classes. However in VI based classification, all the pixels were allotted to some crop class irrespective of their size, and hence contributing for area discrepancy with reference area. Many clusters of waterlogged area having crop during kharif were not considered as kharif during manual digitisation but it was assigned to kharif crop

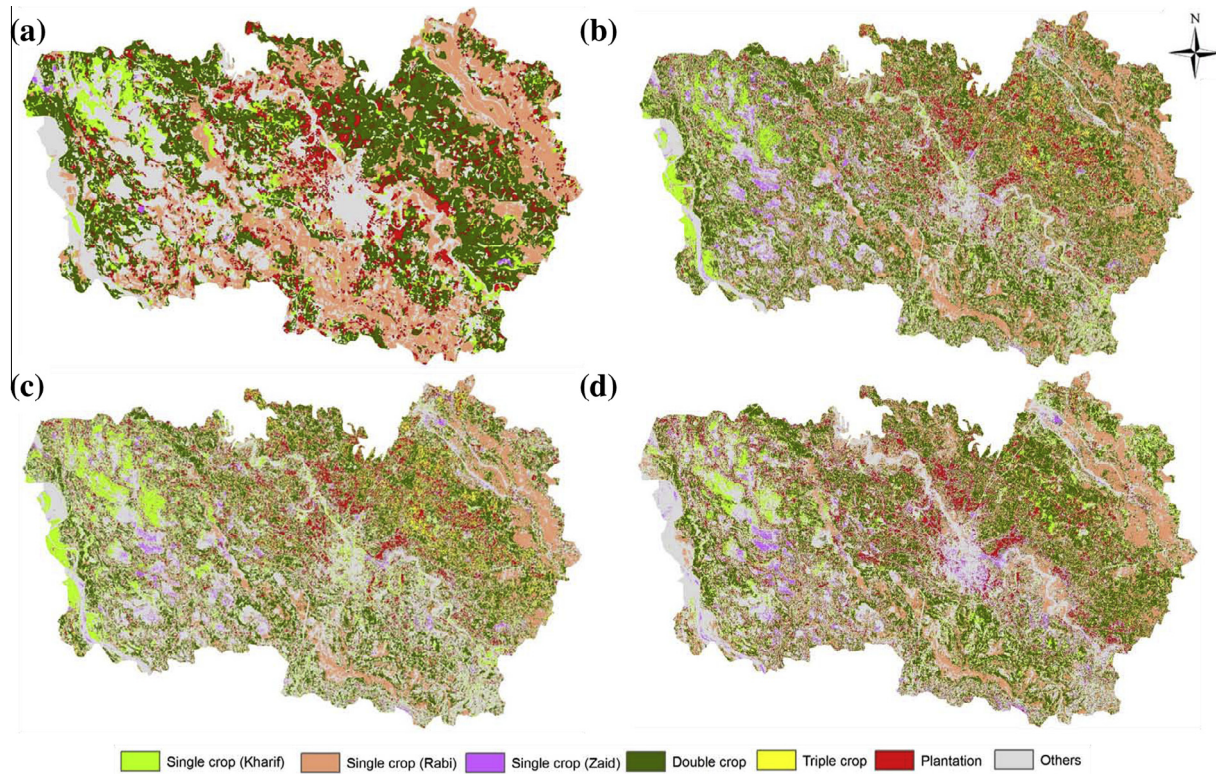


Figure 7 Classified images based on manual digitisation (a) and semi-automated decision tree using NDVI stack (b), EVI2 stack (c) and NDSBVI stack (d).

Table 3 Area estimates from four different mapping approaches.

Class name	Digitised classification (area in Sq. km)	NDVI classification (area in Sq. km)	EVI2 classification (area in Sq. km)	NDSBVI classification (area in Sq. km)
Single crop (kharif)	172.64	196.29	249.28	175.28
Single crop (Rabi)	750.21	358.64	448.56	473.84
Single crop (Zaid)	6.88	93.58	75.95	104.72
Double crop	1008.27	923.01	692.62	823.51
Triple crop	0.00	68.91	113.57	16.39
Plantation	269.35	259.57	256.82	245.5
Total area	2207.35	1900	1836.80	1839.24

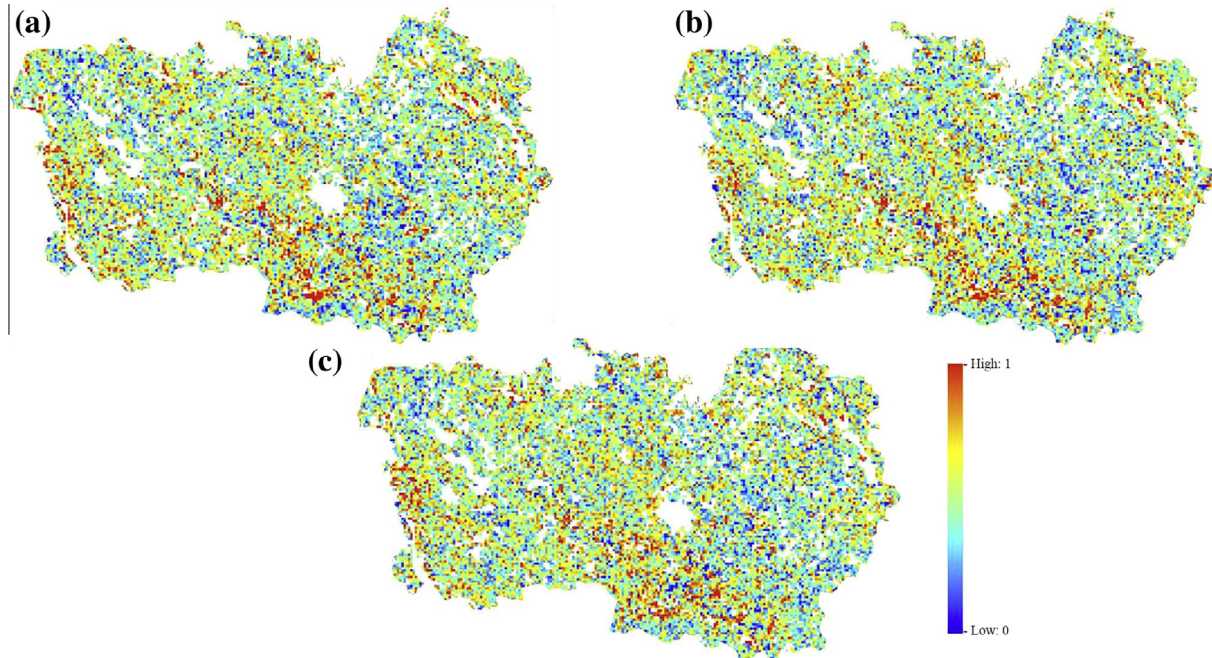
during conditional decision analysis using VI value ranges estimated based on samples. Hence, the kharif crop area was overestimated in all VIs. All the VI based classified maps were very effective in mapping plantation with a high accuracy. Total area of plantation extracted using digitisation technique, NDVI, EVI2 and NDSBVI were 269, 259, 256 and 245 Sq. km, respectively. Though Table 4 reveals the area estimates from classified images using different VI measures, revealing only non-spatial accuracy, it does not provide any clue about the spatial match. In order to estimate spatial match, we have calculated kernel based spatial correlation coefficient (r) between reference-digitised map and a classified map from a VI stack. We have used non-overlapping kernel to determine the spatial match. In addition, the spatial match using different kernel sizes was calculated as to understand the influence of kernel size and accuracy. Table 4 provides the spatial accuracy as a percentage area at different kernel sizes. Fig. 8 reveals the pattern of spatial match over the study area. It could be seen

in Fig. 8 that red colour depicts the highest match and blue colour depicts the lowest match. When the kernel size was small, there was more probability to get a mismatch because in the digitised map the pixel clusters belonging to a class but smaller than MMU were merged with the bigger neighbour class. Since the kernel type considered for calculating correlation was of non-overlapping in nature, it would be appropriate to consider bigger kernel size greater than 15×15 . In this regard, it can be said that overall accuracy of semi-automatic classification using seasonal VI stacks is greater than 53%.

The study found that double seasonal crop and single seasonal (Rabi) crop occupy maximum area of the district. The district has a very good water potential as three main rivers such as Gandak, Burhi Gandak and Bagmati River, are flowing across the study area. Double seasonal crop area was mainly concentrated on the eastern and western part of Burhi Gandak river. Single seasonal (Rabi) crop area was distributed on the eastern part of Bagmati River and Southern side of the

Table 4 Spatial accuracy between reference map and map from other three approaches.

	Spatial accuracy (in % area) at different kernel sizes (in Pixels)			
	15 × 15	21 × 21	41 × 41	51 × 51
Reference digitised map vs. NDVI	52.07	60.80	75.30	80.10
Reference digitised map vs. EVI2	53.44	63.25	79.55	87.93
Reference digitised map vs. NDSBVI	53.55	63.00	80.85	87.30

**Figure 8** Spatial match (correlation within 360 × 360 m kernel) between manually digitised reference map and VI based classified map using NDVI (a), EVI2 (b) and NDSBVI (c) stacks.

district. Most of the plantation areas were located on the central part (around the Muzaffarpur city) of the district. The maximum area of single seasonal (kharif and zaid) crop was identified on the western part of the district close to Gandak River.

5. Conclusion

This study adopted a quick and effective approach utilising seasonal vegetation indices for extracting cropping patterns. Although mixed pixels have contributed for the lower accuracy level of classification, overall information extraction process was effective because seasonal spectral variability effect was nullified by using vegetation indices where the VI value ranges are fixed and different land covers have a characteristic annual VI curve. In this method plantation areas and their extent was also successfully identified with 96%, 95% and 91% accuracy using seasonal stacks of NDVI, EVI2 and NDSBVI, respectively. Among the three VIs, NDVI based approach yielded the lowest accuracy in terms of spatial match with respect to manually digitised reference map. However, the difference in the accuracy levels between the classified maps from these three indices was not much, and hence all the VIs have found to be equally useful in cropping studies. Overall, findings from

the study suggest that semi-automatically delineating the seasonal cropping period and plantation mapping is cost effective and time saving with acceptable accuracy.

Acknowledgement

We would like to express our sincere thanks to the National Remote Sensing Centre (NRSC) and the Indian Space Research Organization (ISRO) for the satellite images.

References

- Bannari, A., Pacheco, A., Staenz, K., McNairn, H., Omari, K., 2006. Estimating and mapping crop residues cover on agricultural lands using hyperspectral and IKONOS data. *Remote Sens Environ.* 4 (104), 447–459.
- Basnyat, P., McConkey, B., Meinert, B., Gatkze, C., Noble, G., 2004. Agriculture field characterization using aerial photograph and satellite imagery. *IEEE Geosci. Remote Sensing Lett.* 1, 7–10.
- Bolton, K.D., Friedl, A.M., 2013. Forecasting crop yield using remotely sensed vegetation indices and crop phenology metrics. *Agric. Forest Meteorol.* 15 (173), 74–84.
- Census of India, 2011. Provisional Population Totals. Office of the Director of Census Operation, Bihar, Patna.

- Central Ground Water Board (CGWB), 2009. Ground Water Information Booklet, Ministry Of Water Resources. Govt. of India, Mid-Eastern Region, Patna.
- Doraiswamy, P.C., Moulin, S., Cook, P.W., Stern, A., 2003. Crop yield assessment from remote sensing. *Photogram. Eng. Remote Sensing*. 69, 665–674.
- Doraiswamy, C.P., Hatfield, L.J., Jackson, J.T., Akhmedov, B., Prueger, J., Stern, A., 2004. Crop condition and yield simulations using Landsat and MODIS. *Remote Sensing Environ.* 4 (92), 548–559.
- FAO, 2009. High Level Expert Forum-How To Feed The World In 2050, Global Agriculture Towards 2050. Economic and Social Development Department, Agricultural Development Economics Division, Rome.
- FAO, 2012. The State of Food Insecurity in the World. Economic growth is necessary but not sufficient to accelerate reduction of hunger and malnutrition. Rome.
- Fang, H., Wu, B., Liu, H., Xuan, H., 1998. Using NOAA AVHRR and Landsat TM to estimate rice area year-by-year. *Int. J. Remote Sensing*. 3, 521–525.
- Fang, H., 1998. Rice crop area estimation of an administrative division in China using remote sensing data. *Int. J. Remote Sensing*. 19 (17), 3411–3419.
- Gallego, J.F., Kussul, N., Skakun, S., Kravchenko, O., Shelestov, A., Kussul, O., 2014. Efficiency assessment of using satellite data for crop area estimation in Ukraine. *Int. J. Appl. Earth Obs. Geoinf.* 29, 22–30.
- Goward, S.N., Davis, E.P., Fleming, D., Miller, L., Townshend, R.J., 2003. Empirical comparison of Landsat 7 and IKONOS multispectral measurements for selected Earth Observation System (EOS) validation sites. *Remote Sensing Environ.* 88, 196–209.
- Hannerz, A.L., 2008. Assessment of remotely sensed and statistical inventories of African agriculture fields. *Int. J. Remote Sensing*. 29 (13), 3787–3804.
- Husak, G.J., Marshall, M.T., Michaelsen, J., Pedreros, D., Funk, C., Galu, G., 2008. Crop area estimation using high and medium resolution satellite imagery in areas with complex topography. *J. Geophys. Res.-Atmos.* 113, D14112.
- IPCC, 2013. Climate Change 2013. The Physical Science Basis. Cambridge University Press, New York.
- Jiang, Z., Huete, A.R., Didan, K., Miura, T., 2008. Development of a two-band enhanced vegetation index without a blue band. *Remote Sensing Environ.* 10 (112), 3833–3845.
- Lamb, W.D., Brown, B.R., 2001. Precision agriculture: remote-sensing and mapping of weeds in crops. *J. Agric. Eng. Res.* 2 (78), 117–125.
- MacDonald, R.B., 1976. Large Area Crop inventory Experiment. In: 2nd Annual William T. Pecora Memorial Symposium, 25–29 October. South Dakota, USA.
- Matthews, E., Fung, I., Lerner, J., 1991. Methane emission from rice cultivation: geographic and seasonal distribution of cultivated areas and emissions. *Global Biogeochem. Cycles.* 5, 3–24.
- Minas, K.P., Dent, F.J., 2002. Lychee Production in the Asia-Pacific Region, Food and Agriculture Organization of the United Nations. Regional Office for Asia and the Pacific, Bangkok, Thailand.
- Mkhabela, M.S., Bullock, P., Raj, S., Wang, S., Yang, Y., 2011. Crop yield forecasting on the Canadian Prairies using MODIS NDVI data. *Agric. Forest Meteorol.* 3 (151), 385–393.
- Moran, S.M., Inoue, Y., Barnes, M.E., 1997. Opportunities and limitations for image-based remote sensing in precision crop management. *Remote Sensing Environ.* 3 (61), 319–346.
- Okamoto, K., Fukuhara, M., 1996. Estimation of paddy rice field area using the area ratio of categories in each pixel of Landsat TM. *Int. J. Remote Sensing*. 9, 1735–1749.
- Okamoto, K., Kawashima, H., 1999. Estimating of rice-planted area in the tropical zone using a combination of optical and microwave satellite sensor data. *Int. J. Remote Sensing*. 5, 1045–1048.
- Panda, S.S., Ames, D.P., Panigrahi, S., 2010. Application of vegetation indices for agricultural crop yield prediction using neural network techniques. *Remote Sensing*. 2, 673–696.
- Panigrahy, S., Sharma, A.S., 1997. Mapping of crop rotation using multiday Indian remote sensing satellite digital data. *ISPRS J. Photogrammetry Remote Sensing*. 2 (52), 85–91.
- Peng, D., Huete, A.R., Huang, J., Sun, H., 2011. Detection and estimation of mixed paddy rice cropping patterns with MODIS data. *Int. J. Appl. Earth Obs. Geoinf.* 13 (1), 13–23.
- Plant, R.E., Munk, D.S., Roberts, B.R., Vargas, R.L., Rains, D.W., Travis, R.L., Hutmacher, R.B., 2000. Relationship between remotely sensed reflectance data and cotton growth and yield. *Trans. ASAE* 43, 535–546.
- Prasad, T.S., Schull, M., Turrall, H., 2005. Ganges and Indus river basin land use/land cover (LULC) and irrigated area mapping using continuous streams of MODIS data. *Remote Sensing Environ.* 95 (3), 314–317.
- Ramankutty, N., 2004. Croplands in West Africa: a geographically explicit dataset for use in models. *Earth Interac.* 8 (23), 1–22.
- Rouse, J.W., Haas, R.H., Schell, J.A., Deering, D.W., 1973. Monitoring vegetation systems in the Great Plains with ERTS. In: 3rd ERTS Symposium. NASA SP-351 I, pp. 309–317.
- Saadat, H., Adamowski, J., Bonnell, R., Sharifi, F., Namdar, M., Ale-Ebrahim, S., 2011. Land use and land cover classification over a large area in Iran based on single date analysis of satellite imagery. *ISPRS J. Photogrammetry Remote Sensing*. 5 (66), 608–619.
- Seelan, K.S., Laguette, S., Casady, M.G., Seielstad, A.G., 2003. Remote sensing applications for precision agriculture: a learning community approach. *Remote Sensing Environ.* 88, 157–169.
- Sha, Z., Bai, Y., Xie, Y., Yu, M., Zhang, L., 2008. Using a hybrid fuzzy classifier (HFC) to map typical grassland vegetation in Xilinhe River Basin, Inner Mongolia, China. *Int. J. Remote Sensing* 8 (29), 2317–2337.
- Son, N.-T., Chen, C.-F., Chen, C.-R., Duc, H.-N., Chang, L.-Y., 2014. A phenology-based classification of time-series modis data for rice crop monitoring in mekong delta Vietnam.. *Remote Sensing*. 6, 135–156.
- SREP, 2011. Strategic Research and Extension Plan, Agriculture Contingency Plan for District: Muzaffarpur. District Agriculture Office, Muzaffarpur, Bihar.
- Sun, J., 2000. Dynamic monitoring and yield estimation of crops by mainly using the remote sensing technique in China. *Photogrammetric Eng. Remote Sensing*. 66, 645–650.
- Taylor, J.C., Wood, G.A., Thomas, G., 1997. Mapping yield potential with remote sensing. *Precision Agriculture*. 1, 713–720.
- Tennakoon, S.B., Murty, V.V.N., Etumnoh, A., 1992. Estimation of cropped area and grain yield of rice using remote sensing data. *Int. J. Remote Sensing*. 13, 427–439.
- Thenkabail, P.S., Ward, A.D., Lyon, J.G., 1995. Landsat-5 Thematic Mapper models of soybean and corn crop characteristics. *Int. J. Remote Sensing*. 15, 49–61.
- Toan, L.T., Ribbes, F., Wang, L., Flouri, N., Ding, K., Kong, A.J., Fujita, M., Kurosu, T., 1997. Rice crop mapping and monitoring using ERS-1 data based on experiment and modelling results. *IEEE Trans. Geosci. Remote Sensing*. 1 (35), 41–56.
- UNFPA, 2012. State of World Population. United Nation Population Fund, New York.
- USCB, 2004. International Population Reports WP/02, Global Population Profile: 2002. U.S. Government Printing Office, Washington, DC.
- Xiao, X., He, L., Salas, W., Li, C., Moore, B., Zhao, R., 2002a. Quantitative relationships between field-measured leaf area index and vegetation index derived from VEGETATION images for paddy rice fields. *Int. J. Remote Sensing*. 23, 3595–3604.
- Xiao, X., Boles, S., Frolik, S., Salas, W., Moore, B., Li, C., 2002b. Landscape-scale characterization of cropland in China using

- Vegetation and Landsat TM images. *Int. J. Remote Sensing.* 23, 3579–3594.
- Xiao, X., Boles, S., Frolking, S., Li, C., Babu, J.Y., Salas, W., Moore, B., 2006. Mapping paddy rice agriculture in South and Southeast Asia using multi-temporal MODIS images. *Remote Sensing Environ.* 100 (1), 95–113.
- Xin, J., Yu, Z., Leeuwen, V.L., Driessen, M.P., 2002. Mapping crop key phenological stages in the North China Plain using NOAA time series images. *Int. J. Appl. Earth Obs. Geoinf.* 2 (4), 109–117.
- Yang, C., Anderson, G.L., 2000. Mapping grain sorghum yield variability using airborne digital videography. *Precis. Agric.* 2, 7–23.
- Yang, C., Everitt, H.J., Murden, D., 2011. Evaluating high resolution SPOT 5 satellite imagery for crop identification. *Comput. Electron. Agric.* 2 (75), 347–354.
- Zhang, J., Foody, G.M., 1998. A fuzzy Classification of sub-urban land cover from remotely sensed imagery. *Int. J. Remote Sensing.* 19, 2721–2738.
- Van Niel, G.T., McVicar, R.T., 2004. Determining temporal windows for crop discrimination with remote sensing: a case study in south-eastern Australia. *Comput. Electron. Agric.* 45, s1–s3 (91–108).